

Measurements of electron-impact ionization cross sections of argon, krypton, and xenon by comparison with photoionization

A. A. Sorokin, L. A. Shmaenok,* and S. V. Bobashev

A. F. Ioffe Physico-Technical Institute RAS, Politekhnicheskaya 26, 194021 St. Petersburg, Russia

B. Möbus, M. Richter, and G. Ulm

Physikalisch-Technische Bundesanstalt, Abbestraße 2-12, 10587 Berlin, Germany

(Received 15 July 1999; published 18 January 2000)

Ratios of total cross sections for electron-impact ionization and photoionization in Ar, Kr, and Xe in the energy range from 140 to 4000 eV for electrons and from 16 to 1012 eV for photons were measured. Comparatively low relative standard uncertainties of 1.3–1.9% were achieved using an apparatus combining two recent instrumental developments. The first is associated with a highly accurate device for the determination of soft-x-ray and vacuum-UV photon flux, a cryogenic electrical substitution radiometer. The second is an upgraded ionization chamber for the precise comparison of total-ion yields for electron and photon impact. On the basis of our measured cross-section ratios and well-known total photoionization cross-section data, we deduced absolute total electron-impact ionization cross sections of the rare gases with relative standard uncertainties as low as 2%.

PACS number(s): 32.80.Fb, 34.80.Dp

I. INTRODUCTION

Electron-impact ionization (EI) and photoionization (PI) are two fundamental processes in atomic and molecular physics. Experimental cross-section data for these processes with low uncertainties are of great interest from the point of view of both theory and application. Numerous measurements of total and partial cross sections of rare gases, which are the most popular targets, have been reported in the literature for EI and PI for many years. However, the situation as regards accurate cross-section data significantly differs for the two ionization processes. While relative uncertainties of measured PI cross sections have been reduced to 0.8–3%, relative uncertainties quoted for measured EI cross sections typically range between 6% and 15%.

In a recent paper [1] we reported on a new method for the determination of total EI cross sections of rare gases. The method is based on the accurate measurement of ratios of total cross sections for EI and PI, followed by the determination of the total EI cross sections using the measured cross-section ratios and well-known total PI cross sections. For a practical application of the method, we developed an ionization chamber in which the total-ion yields by photon and electron impact can be accurately compared. Using photodiodes calibrated against a cryogenic electrical substitution radiometer (ESR) as the primary detector standard in the spectral range of vacuum-UV (VUV) radiation and soft x rays, the impact photon flux could be measured with relative standard uncertainties below 1% [2,3]. Based on this progress achieved in the measurement of photon flux and of ion yield ratios, relative standard uncertainties for the cross-section ratios as low as 1.3% are attainable at present. Our

recent measurements of ratios of EI and PI cross sections performed in the soft-x-ray photon energy range and of absolute total EI cross sections in the energy range of electrons from 140 to 4000 eV on Ne [1] have demonstrated the high reliability of the method and its suitability for EI cross-section measurements on other rare gases.

In the present work, the measurements were extended to Ar, Kr, and Xe and to the VUV photon energy range. We present ratios of EI cross sections and PI cross sections as well as absolute total EI cross sections for these rare-gas atoms in the energy range from 140 to 4000 eV for electrons and from 16 to 1012 eV for photons. Relative standard uncertainties as low as 1.3–1.9% for the cross-section ratios and of 2% for the total EI cross sections were achieved. Our results considerably improve the database for absolute total EI cross sections and hence for partial cross sections derived from these data.

II. APPARATUS AND EXPERIMENTAL DETAILS

The measurements were performed in the radiometry laboratory of the Physikalisch-Technische Bundesanstalt at the Berliner Elektronenspeicherrung-Gesellschaft für Synchrotron-strahlung (BESSY I). Two beamlines in this laboratory were used to cover the photon energy range of interest. The SX700 beamline equipped with an SX700 plane grating monochromator and a toroidal refocusing mirror behind the exit slit 200 μm in width was utilized in the photon energy range from 50 to 1012 eV [4]. Measurements at photon energies of 16.7, 16.9, and 21.2 eV (the choice of just these spectral points is discussed in Sec. III) were performed at the normal-incidence monochromator (NIM) beamline. The NIM beamline contained an SiC premirror and a 1-m normal-incidence 15° McPherson-type monochromator equipped with SiC spherical gratings [2,5]. In order to obtain a high intensity of the radiation required for the measurements, the entrance and exit slits of this monochromator were fixed at 1 mm in width. Under these conditions, a pho-

*Present address: Phystex, Dukatenburg 30b, 3437 AC Nieuwegein, The Netherlands.

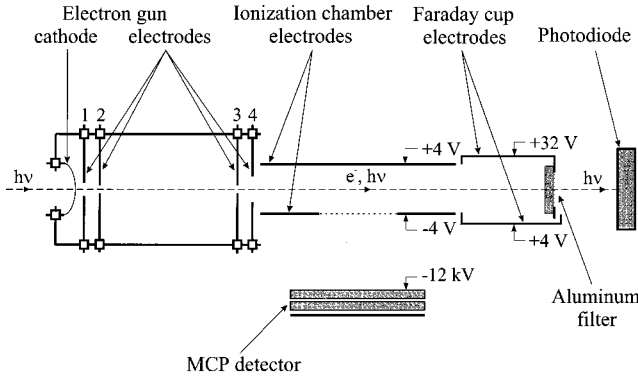


FIG. 1. Scheme of the apparatus.

ton flux of up to 10^{12} s^{-1} and a resolving power $\lambda/\Delta\lambda$ of approximately 90 were available at the NIM beamline. The corresponding values for the SX700 beamline were 10^{11} s^{-1} and 300, respectively.

The apparatus used for the cross-section measurements (Fig. 1) as well as the experimental procedure for measurements at the SX700 beamline were discussed in detail previously [1]. Briefly, the target rare gas of 99.99% or better purity homogeneously fills the ionization chamber. Its pressure is maintained at certain levels in the range between 2×10^{-4} and 3×10^{-3} Pa during the measurements. The operation of the apparatus is based on the successive ionization of the target gas by electrons and photons under identical conditions and on the comparison of the corresponding ion yields. In the first step, a beam of monoenergetic electrons of energy E is directed between two parallel electrodes of the ionization chamber, and collected in a Faraday cup. Through a grid-covered aperture ($3.4 \times 3.4 \text{ cm}^2$) in the bottom electrode, a fraction of positive ions is extracted by a static electric field of 5 V/cm into the gap between the electrode and the front area of a microchannel plate MCP detector. In this section, the ions are accelerated by a voltage of 12 kV before being registered by the MCP detector. In the second step, the electron beam is stopped and a beam of monochromatized synchrotron radiation of photon energy $h\nu$ enters the ionization chamber through the hollow-axis electron gun, passes through the aperture at the bottom of the Faraday cup, covered with a $0.15\text{-}\mu\text{m}$ -thick aluminum filter of known transmittance, and is detected by a calibrated silicon *n-on-p* photodiode [International Radiation Detectors (IRD), AXUV 100G]. The ions created by PI are collected and registered as in the case of EI. The design of the apparatus utilizing the hollow-axis electron gun and the thin aluminum filter at the bottom of the Faraday cup ensures the coincidence of the photon and electron-beam trajectories in the ionization chamber, and allows EI and PI measurements to be performed without any change in the position of the electron gun and Faraday cup. This guarantees equivalent conditions for EI and PI as regards the gas density and the electric potential distribution within the ionization chamber. Moreover, because the ion extraction and accelerating fields are chosen high enough to obtain equal collection and detection efficiency for differently charged ions, the ratio of total EI

cross section $\sigma_e(E)$ to total PI cross section $\sigma_{\text{ph}}(h\nu)$ can be expressed by [1]:

$$\frac{\sigma_e(E)}{\sigma_{\text{ph}}(h\nu)} = \frac{1}{\tau_{\text{ph}}(h\nu)} \cdot \frac{1}{\eta_{\text{ph}}(h\nu)} \frac{f_e/I_e}{f_{\text{ph}}/I_{\text{ph}}}. \quad (1)$$

I_e and I_{ph} denote the current of Faraday cup and photodiode, respectively; f_e and f_{ph} are the MCP detector count rates for ions formed by electron and photon impact, respectively; $\tau_{\text{ph}}(h\nu)$ is the transmittance of the aluminum filter; and $\eta_{\text{ph}}(h\nu)$ is the quantum efficiency of the photodiode. The absolute determination of all quantities on the right-hand side of Eq. (1), as well as the analysis of the respective contributions to the total relative uncertainties of the cross-section ratios, were performed in the soft-x-ray spectral range for each rare gas, as has been done in our previous work for Ne [1].

Owing to a number of special features of the measurements in the VUV spectral range, the experimental procedure and the apparatus used at the NIM beamline underwent several changes. In the following, we discuss these changes and analyze the respective contributions to the total relative uncertainty of the cross-section ratios due to these changes.

First, because of a considerable reflectance of photons on surfaces in the energy range of the NIM, a Faraday cup covered with an aluminum filter at its bottom was not suited for the measurements at the NIM beamline. Otherwise a fraction of photons reflected backwards from the filter might have led to an additional undesirable creation of ions and their registration by the MCP detector. In order to eliminate this problem, we used two slightly different Faraday cups for the EI and PI measurements. The aperture at the bottom of the first cup for EI was covered with an aluminum filter, that of the second one for PI (not shown in Fig. 1) was open. Both Faraday cups were mounted on a linear-motion feedthrough, and could therefore be replaced during the measurements. In order to test if the replacement of the Faraday cups between EI and PI measurements disturbs the gas density and the electric potential distribution within the ionization chamber and if it influences, as a result, ion production and collection, we measured the ion count rate during EI while the Faraday cups were replaced. However, we did not observe any significant effect beyond 0.2%.

The second distinguishing feature of the measurements at the NIM beamline was the use of a trap detector instead of an *n-on-p* IRD AXUV 100 G photodiode for the determination of the photon flux. The trap detector consisted of three PtSi-*n*-Si Schottky barrier photodiodes known to be most suitable for use in the VUV spectral range due to their high stability under prolonged radiant exposure [6]. The photodiodes used in the trap detector were mounted such with respect to each other that the incoming photon beam had to undergo five reflections from photodiodes to be reflected backwards. With this design, photon reflection from the trap detector has been found to be negligible in test measurements. The currents from these photodiodes were added up and measured with a relative uncertainty of 0.1% by the same Keithley 617 picoammeter as used for the electron current. Typical values of the photocurrent ranged from 2 to 4 nA, depending on the photon flux. The dark current of the trap detector was in the range of 100 pA, and remained stable within 10 pA during individual cross-section measurements.

The dark current was subtracted from the total current, resulting in the true trap detector photocurrent I_{ph} . The fluctuation of the dark current determines an upper limit of 0.3% for the contribution from the dark current correction to the total relative uncertainty of our cross-section measurements. By calibration against the ESR as primary detector standard [2,3], the quantum efficiency $\eta_{\text{ph}}(h\nu)$ of the trap detector was determined with a relative standard uncertainty of 1.5%. An additional uncertainty of 0.2% for the determination of the photon flux at the NIM beamline came from the uncertainty of the NIM energy calibration.

Moreover, during the PI measurements at the NIM beamline, both the ion count rate and the trap detector current were affected by higher-order radiation and stray light [7]. In the higher-order spectrum of the NIM beamline, second-order radiation was predominant. In order to reduce second-order radiation, a 4-m-long gas filter was used, filled with Ne at a pressure of 2 Pa and separated from our apparatus by a system of differential pumping units. Remaining second-order contribution and its influence on the cross-section measurements was determined by test experiments at different pressures of Ne in the gas filter. Using data in the whole spectral range from 10 to 35 eV, for the PI cross sections of the working rare gas from literature (see the references mentioned in Sec. III), respectively, and for the quantum efficiency of the trap detector obtained by calibration against the ESR, we found the ratio of second-to-first-order photons to be negligible at the photon energy of 21.2 eV. At 16.7 and 16.9 eV, we measured the remaining contribution of second order to be 0.7%, resulting in a second-order correction of the measured cross-section ratios of 5% and a respective contribution to the total relative uncertainty of our cross-section measurements of 0.5%.

In the spectral range between 10 and 35 eV, stray light photons with photon energies above 5 eV were recently found to be negligible at the NIM beamline [7]. In order to check the influence of low-energy stray light, we introduced an MgF_2 window into the beam, mounted on a linear-motion feedthrough, which effectively cut off radiation with photon energies above 11 eV while it was transparent below. In this way, at the photon energies of 16.7, 16.9, and 21.2 eV we measured the remaining trap detector current of stray light photons below 11 eV to be less than 0.3% of the total current, the latter being obtained without the MgF_2 window. Since these low-energy photons do not affect the rare-gas ionization at all but only the trap detector current, we conclude that the upper limit of the influence of low-energy stray light on our cross-section measurements was also less than 0.3%.

III. RESULTS AND DISCUSSION

Ratios $\sigma_e(E)/\sigma_{\text{ph}}(h\nu)$ of total cross sections for EI and PI of Ar, Kr, and Xe were measured at an electron energy E of 1000 eV and selected photon energies $h\nu$ between 16 and 1012 eV. In order to avoid additional errors, we chose the photon energies for each target rare gas within regimes without absorption edges and resonance structures in the respective photoionization spectrum. Moreover, the measurements

were performed only at photon energies for which experimental data for total PI cross sections are available in the literature. The cross-section ratios were measured during two different periods within two years. The two sets of data thus obtained agreed within the combined relative uncertainties. The average results of these measurements are presented in Table II. The contributions to the total relative standard uncertainties of the ratios partly discussed above (for more details, see Ref. [1]) are summarized in Table I.

The total EI cross sections at 1000-eV electron energy were deduced from the measured ratios by normalization to absolute total PI cross sections reported in the literature by different experimental groups. We selected results only of those groups which reported original PI cross-section data measured after 1960 with quoted relative uncertainties better than 7%, using all experimental techniques available [8]. Results of compilations are not discussed. Accordingly, in the spectral range covered by the SX700 beamline (i.e., in the photon energy range from 50 to 1012 eV), we used data reported by Samson *et al.* [9] and obtained by the double-ionization chamber technique with a quoted relative uncertainty of 3% for the PI cross sections of Ar, Kr, and Xe, as well as data reported by Yang and Kirz [10] (Ar, 1.5%), Watson [11] (Ar, 3%), Denne [12] (Ar, 2%), Henke *et al.* [13] (Ar, Kr, and Xe, 3%), Wuilleumier [14] (Ar, Kr, and Xe, 5% to 7%), and Lang and Watson [15] (Kr and Xe, 5%), obtained by the absorption cell technique. In the spectral range covered by the NIM beamline we used PI cross-section data reported by Samson and Yin [16] for Ar, Kr, and Xe at photon energies of 16.7, 16.9, and 21.2 eV only, obtained by the double-ionization chamber technique with a quoted relative uncertainty of 0.8%. Results of other experimental groups available from literature for the latter spectral range were not taken into consideration because they agree, in most cases, within combined relative uncertainties with those reported by Samson and Yin, which are of significantly higher accuracy (see Ref. [16], and references therein). The deduced total EI cross sections are plotted in Figs. 2–4. The relative uncertainties arise from the relative uncertainties of the measured ratios and the relative uncertainties of the absolute total PI cross sections claimed by the authors.

In the case of Ar (Fig. 2), values for the total EI cross section deduced by normalization to the most accurate total PI cross sections reported by Samson and co-workers [9,16], Yang and Kirz [10], and Denne [12] are in excellent agreement with one another. Averaging of these values results in a total EI cross section of Ar $\sigma_e(E=1000\text{ eV})=80.8\text{ Mb}$ with a relative standard uncertainty of 2%. EI cross-section values deduced by normalization to the less accurate PI cross sections reported by Watson [11], Henke *et al.* [13], and Wuilleumier [14] and obtained with slightly higher relative uncertainties of 3.3–5.3%, demonstrate larger diversity. Nevertheless, these data agree within combined relative uncertainties with the average value for $\sigma_e(E=1000\text{ eV})$. The agreement of our results for $\sigma_e(E=1000\text{ eV})$ obtained at different photon energies by normalization to the different sets of PI cross-section data demonstrates both the high reliability of the PI cross-section data and again, as for Ne [1], the consistency of our method. In particular, it confirms that

TABLE I. Contributions to the relative standard uncertainty of the ratios of the total cross sections for electron-impact ionization and photoionization of Ar, Kr, and Xe at 1000-eV electron energy and photon energies $h\nu$ ranging from 16 to 1012 eV.

Source of uncertainty	Contributions to the relative standard uncertainty of total cross-section ratios (%)	
	16 eV $\leq h\nu \leq$ 21.2 eV	50 eV $\leq h\nu \leq$ 1012 eV
Current of impact electrons	0.2	0.2
Energy of impact electrons	0.1	0.1
Number of impact photons		
Photodiode current	0.1	0.1
Dark current correction	0.3	-
Aluminum filter transmittance	-	0.2
Photodiode quantum efficiency	1.5	0.8
Energy of impact photons	0.2	0.2–0.4
Count rate measurements		
Counting statistics	0.5	0.5
Background correction	0.2	0.1–0.4
Linearity of detector	0.5	0.5
Equivalence of interaction path lengths	0.1	0.1
Equivalence of ion collection efficiencies	0.5	0.5
Equivalence of ion detection efficiencies	0.1	0.1–0.5
Gas pressure stability	0.1	0.1
Effects by secondary electrons ^a	0.3	0.3
Second-order contribution	0.1–0.5	0.1–0.5
Stray light contribution	0.3	0.2–1.0
Total relative uncertainty (sum in quadrature)	1.8–1.9	1.3–1.8

^aSee the discussion in Ref. [1].

our method is insensitive to the strong enhancement of the fraction of multiply charged ions (predominantly doubly charged) by PI near the $2p$ threshold of Ar ($h\nu \cong 248$ eV) [17] (the influence of multiply charged ions on our measurements has been previously discussed in detail [1]).

In the case of Kr (Fig. 3), values for the total EI cross section deduced by normalization to the PI cross sections reported by Samson and co-workers [9,16], Henke *et al.* [13], and Wuilleumier [14] are again in very good agreement with one another, demonstrating that the PI cross-section data are reliable and that our measurements are not affected by the severe change in the ion charge spectrum for PI at the $3d$ threshold of Kr ($h\nu \cong 95$ eV) [17]. The values deduced by normalization to the PI cross sections reported by Lang and Watson [15] are slightly higher than the other ones, and show greater scatter. We note that the measurements performed at the SX700 beamline and, therefore, based on the PI cross-section data reported in Refs. [9,13–15], result in values for the total EI cross section with relative standard uncertainties ranging between 3.3% and 5.3%, whereas the measurements performed at the NIM beamline are associated with a significantly lower relative standard uncertainty of 2%. Therefore, we rely only on the latter measurements and come to a total EI cross section of Kr $\sigma_e(E$

$= 1000$ eV) $= 106.2$ Mb with a relative standard uncertainty of 2%.

In the case of Xe (Fig. 4), to derive the total EI cross section at an electron energy of 1000 eV, we again rely on the most accurate results obtained at the NIM beamline at the photon energies of 16.7 and 16.9 eV. Measurements at a photon energy of 21.2 eV were not performed since this spectral point lies in a region containing resonance structures [18]. We come to a value $\sigma_e(E = 1000$ eV) $= 143.7$ Mb with a relative standard uncertainty of 2%. The measurements performed at the SX700 beamline reveal considerable discrepancies in the magnitude of the total EI cross section deduced by normalization to the different sets of PI cross-section data. Only the results obtained with a relative uncertainty of 3.3% by normalization to the PI cross sections reported by Samson *et al.* [9] are in good agreement with those obtained at the NIM beamline, confirming the reliability of the latter. Values for the total EI cross section deduced by normalization to the less accurate PI cross sections reported by Henke *et al.* [13], Wuilleumier [14], and Lang and Watson [15] agree within combined uncertainties with the value for $\sigma_e(E = 1000$ eV) in the photon energy range from 116 to 525 eV, whereas in the other spectral ranges the data differ by up

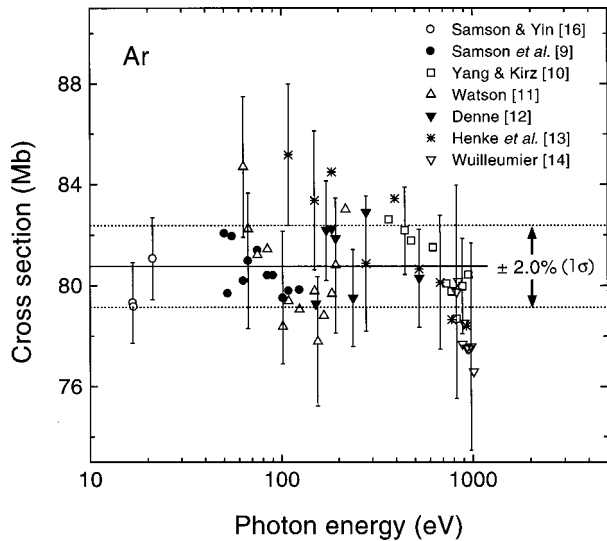


FIG. 2. Total electron-impact ionization cross section of Ar at an electron energy of 1000 eV obtained from measured cross-section ratios and normalization to total photoionization cross sections at different photon energies. Different symbols represent data obtained by normalization to different sets of photoionization cross-section data [9–14,16]. The continuous line represents the average value (see the text). The representative uncertainty bars at selected energies correspond to the relative standard uncertainties mentioned in Sec. III.

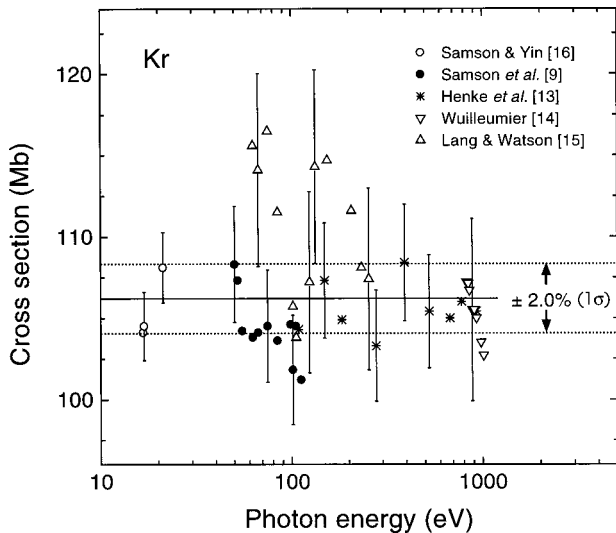


FIG. 3. Total electron-impact ionization cross section of Kr at an electron energy of 1000 eV obtained from measured cross-section ratios and normalization to total photoionization cross sections at different photon energies. Different symbols represent data obtained by normalization to different sets of photoionization cross-section data [9,13–16]. The continuous line represents the average value (see the text). The representative uncertainty bars at selected energies correspond to the relative standard uncertainties mentioned in Sec. III.

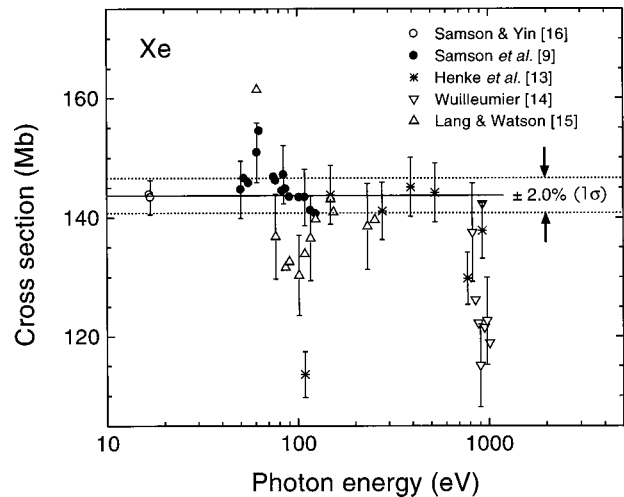


FIG. 4. Total electron-impact ionization cross section of Xe at an electron energy of 1000 eV obtained from measured cross-section ratios and normalization to total photoionization cross sections at different photon energies. Different symbols represent data obtained by normalization to different sets of photoionization cross-section data [9,13–16]. The continuous line represents the average value (see the text). The representative uncertainty bars at selected energies correspond to the relative standard uncertainties mentioned in Sec. III.

to 21% (see, for example, the data scattering at 108.8- and 904-eV photon energies).¹ (See Fig. 4.) The confidence in our data is based on the fact that, again as in the case of Ar and Kr, an influence of the strong enhancement of the fraction of multiply charged ions in the ion charge spectrum for PI arising at the $4d$ threshold of Xe ($h\nu \cong 69$ eV) [17] is not observed.

Next, we determined the relative energy dependence of the total EI cross sections of Ar, Kr, and Xe with a relative uncertainty of 1% by comparing ion count rates normalized to the impact-electron current at the reference energy of 1000 eV and at electron energies E between 140 and 4000 eV. Finally, using the absolute value for $\sigma_e(E=1000$ eV), we converted the relative energy dependence into absolute total EI cross sections $\sigma_e(E)$ of Ar, Kr, and Xe, as given in Table III. In Figs. 5–7 we compare our results with published experimental data obtained by direct absolute measurements. Relative measurements normalized to the work of others are omitted. The fractional deviation of these data from the present data is also shown to facilitate comparison. The results of Wetzel *et al.* [19], Straub *et al.* [20], Ma, Sporteder and Bonham [21], Nagy, Skutlartz, and Schmidt [22], Gaudin and Hagemann [23], and Schram *et al.* [24] correspond,

¹In the case of Xe and Kr, our measurements allow the PI cross-section data to be improved in the energy range of photons from 50 to 1012 eV. Taking our measured values for the cross-section ratios (Table II) and the values for $\sigma_e(E=1000$ eV) (see text), one can easily deduce total PI cross sections of Xe and Kr in the photon energy range from 50 to 1012 eV with relative standard uncertainties of 2.4% to 2.7%, i.e., with uncertainties smaller than those reported in the literature for this spectral range.

TABLE II. Ratios of total cross sections obtained for electron-impact ionization and photoionization in Ar, Kr, and Xe. The relative standard uncertainties of the cross-section ratios are indicated in parentheses.

Photon energy $h\nu$ (eV)	$\sigma_e(E=1000 \text{ eV})$		
	Ar	$\frac{\sigma_{\text{ph}}(h\nu)}{\text{Kr}}$	Xe
16.7	2.455(1.9%)	2.318(1.9%)	2.734(1.9%)
16.9	2.424(1.9%)	2.329(1.9%)	2.764(1.9%)
21.2	2.253(1.8%)	2.821(1.8%)	-
50.20	109.4(1.5%)	81.9(1.5%)	111.3(1.7%)
52.20	98.0(1.5%)	97.2(1.4%)	115.9(1.7%)
55.10	86.8(1.4%)	118.4(1.4%)	117.7(1.6%)
61.10	-	-	118.8(1.5%)
62.50	-	167.1(1.4%)	-
62.90	-	-	115.3(1.5%)
63.10	67.2(1.4%)	-	-
66.80	61.89(1.4%)	184.7(1.4%)	-
74.90	58.18(1.3%)	203.3(1.7%)	21.13(1.4%)
76.60	-	-	16.71(1.4%)
82.60	-	-	9.83(1.4%)
84.30	57.73(1.3%)	202.4(1.7%)	8.80(1.4%)
86.30	-	-	7.32(1.4%)
90.40	58.93(1.3%)	-	5.977(1.4%)
98.90	-	82.8(1.5%)	-
101.7	62.12(1.3%)	77.4(1.5%)	5.116(1.4%)
105.7	-	67.9(1.5%)	-
108.8	66.05(1.3%)	57.67(1.4%)	5.989(1.4%)
112.4	-	52.20(1.4%)	-
116.6	-	-	8.28(1.6%)
124.2	75.2(1.3%)	35.84(1.4%)	12.90(1.7%)
133.3	-	28.98(1.4%)	-
148.7	99.0(1.3%)	23.80(1.4%)	64.68(1.8%)
151.0	101.5(1.3%)	-	-
154.4	-	22.50(1.4%)	85.1(1.8%)
154.9	105.4(1.3%)	-	-
166.9	118.3(1.3%)	-	-
171.7	124.5(1.3%)	-	-
183.4	138.9(1.3%)	21.06(1.4%)	-
192.6	150.7(1.3%)	-	-
206.0	-	20.97(1.4%)	-
217.2	186.7(1.3%)	-	-
232.2	-	20.31(1.5%)	103.7(1.6%)
236.9	220.9(1.4%)	-	-
254.1	-	21.54(1.5%)	93.5(1.5%)
277.4	26.73(1.4%)	23.62(1.4%)	90.8(1.5%)
364.7	36.57(1.4%)	-	-
392.4	41.72(1.4%)	36.27(1.4%)	107.3(1.5%)
442.8	53.81(1.4%)	-	-
476.9	62.67(1.4%)	-	-
524.9	76.5(1.4%)	61.63(1.4%)	155.6(1.5%)
619.9	110.6(1.4%)	-	-
676.8	135.1(1.5%)	103.8(1.4%)	-
727.6	158.6(1.7%)	-	-
776.2	185.5(1.7%)	139.8(1.7%)	54.61(1.7%)
825.0	215.6(1.7%)	160.9(1.7%)	61.05(1.7%)

TABLE II. (*Continued*).

Photon energy $h\nu$ (eV)	$\sigma_e(E=1000 \text{ eV})$		
	Ar	$\sigma_{\text{ph}}(h\nu)$ Kr	Xe
841.5	228.4(1.7%)	169.7(1.7%)	-
852.0	-	174.4(1.7%)	-
853.1	-	-	64.15(1.7%)
883.1	253.9(1.7%)	188.8(1.7%)	67.9(1.7%)
904.0	272.4(1.7%)	200.2(1.7%)	69.3(1.7%)
929.7	290.4(1.7%)	213.3(1.7%)	71.8(1.7%)
950.8	307.0(1.7%)	-	66.8(1.7%)
981.8	335.8(1.7%)	241.9(1.7%)	70.9(1.7%)
1012	361.0(1.7%)	258.7(1.7%)	71.2(1.7%)

like ours, to total ionization cross sections σ_e as the sum of all partial cross sections σ^{n+} for the creation of differently charged ions:

$$\sigma_e = \sigma^+ + \sigma^{2+} + \sigma^{3+} + \dots \quad (2)$$

The measurements of Fletcher and Cowling [25], Rapp and Englander-Golden [26], and Smith [27] provided so-called gross ionization cross sections σ_{gross} . This value is the charged-weighted sum of the partial cross sections:

$$\sigma_{\text{gross}} = \sigma^+ + 2\sigma^{2+} + 3\sigma^{3+} + \dots \quad (3)$$

We recalculated the latter data to total ionization cross sections σ_e using ratios $\sigma_{\text{gross}}/\sigma_e$ reported in Ref. [28] with relative uncertainties of 1% for Ar, of 5% for Kr, and 10% for Xe.

We do not enumerate all discrepancies in the absolute cross-section data reported by the different experimental groups, since the details can be seen directly from Figs. 5–7. Moreover, we do not examine each experimental work with respect to possible error sources because this has already been done in the literature (see, for example, the review articles [29,30] as well as in recent experimental work [1,20]). We note only that quoted relative uncertainties of the measured cross sections typically range from 6% to 15%, and the main contributions to them arise from the absolute measurement of (a) the number of impact electrons, (b) the number (or current when gross ionization cross sections are measured) of ions created, (c) the interaction path length accepted from the ion detector, (d) the detector efficiency for differently charged ions, and (e) the target gas density at a pressure of less than 10^{-2} Pa, which is typical of EI experiments employing the most popular beam-static-gas technique [20–27] (in experiments employing a cross-beam technique [19], the latter problem is replaced by the problem of neutral-beam flux measurements).

The present measurements are free of errors associated with the absolute pressure measurements, i.e. with that of (e), and the PI cross-section data used in our normalization procedure were obtained by techniques using gas pressures in the order of 100 Pa, where the application of precision oil

manometers and capacitor manometers allows one to reduce the relative uncertainty of the target gas density to less than 1%, independently of the sort of the gas [16]. Moreover, our measurements allow problems concerning the determination of (a), (b), (c), and (d) to be avoided, since both the present cross-section ratios and the PI cross sections (see, e.g., Refs. [9], [16]) were obtained by means of measurements which do not require absolute determination of these. All this enabled us to determine the total EI cross sections with lowest relative uncertainties.

Until quite recently the results reported by Rapp and Englander-Golden [26], with a quoted relative uncertainty of 7%, were considered *de facto* as a standard, and often used to normalize relative partial cross sections [31–35]. However, in our previous work [1], we obtained total EI cross sections of Ne lower than those reported by Rapp and Englander-Golden by up to 19%. Moreover, our data for Ne were found to be in good agreement with those reported by Schram *et al.* [24], who claimed the relative uncertainty of their cross sections to be 6%. We would like to stress that these are the only groups which measured the absolute cross sections for all rare gases with a quoted relative uncertainty of less than 10% over a wide range of electron energies. Moreover, we concentrate our attention on measurements of just these groups because the disagreements between their results point most clearly to the problems associated with the target gas density determination inherent in the EI cross-section measurements. Indeed, the two groups used a similar techniques based on the measurement of the total ion yield produced by an electron beam passing through a well-defined layer of gas in a beam-static-gas configuration, but utilized different methods to determine the target gas density (see also the discussion in Ref. [1]).

In the present work we find our results for Ar to be in excellent agreement with those reported by both Schram *et al.* [24] and Rapp and Englander-Golden [26], while for Kr and Xe our data are smaller than those obtained by the other two groups. However, within combined relative uncertainties, our cross-section data of Kr agree with those reported by Schram *et al.*, whereas in the case of Xe our data confirm those of Rapp and Englander-Golden. As for relative

TABLE III. Total electron-impact ionization cross sections $\sigma_e(E)$ of Ar, Kr, and Xe, and their relative standard uncertainties.

Electron energy E (eV)	$\sigma_e(E)$ (Mb)			Relative standard uncertainty (%)
	Ar	Kr	Xe	
140	244.1	320.8	445.5	2.2
160	235.0	306.7	422.5	2.2
180	224.4	292.5	401.9	2.2
200	215.9	280.5	383.0	2.1
225	205.1	265.7	361.3	2.1
250	195.3	252.9	342.7	2.1
300	177.2	230.7	311.5	2.1
350	163.0	212.0	286.7	2.1
400	150.6	196.4	265.7	2.1
450	140.6	182.8	247.9	2.1
500	131.2	170.8	231.2	2.1
550	123.4	160.8	217.9	2.1
600	116.4	152.1	205.8	2.1
650	110.0	144.1	194.9	2.1
700	104.5	136.7	184.9	2.1
750	99.6	130.3	176.0	2.1
800	94.9	124.4	168.1	2.1
850	91.0	119.2	161.2	2.1
900	87.4	114.6	154.9	2.1
950	83.9	110.3	149.2	2.1
1000	80.8	106.2	143.7	2.0
1100	75.2	98.7	134.1	2.1
1200	70.4	92.7	125.8	2.1
1300	66.2	87.2	118.5	2.1
1400	62.75	82.7	112.0	2.1
1500	59.50	78.5	106.5	2.1
1600	56.62	74.7	101.6	2.1
1700	54.00	71.4	96.8	2.1
1800	51.66	68.4	92.6	2.1
1900	49.72	65.52	88.7	2.1
2000	47.63	63.01	85.3	2.1
2500	39.91	52.96	71.9	2.1
3000	34.52	45.97	62.26	2.1
3500	30.52	40.50	55.14	2.1
4000	27.39	36.35	49.72	2.1

energy dependencies of the cross sections, we find very good agreement within 2% between our data and those reported by the two groups for Ar, while in the case of Kr and Xe, discrepancies in the energy dependencies of up to 6% occur.

Recently, Straub *et al.* [20] used an apparatus equipped with a time-of-flight mass spectrometer with position-sensitive detection of differently charged ions to measure partial and total EI cross sections of Ar. The improvements in particle detection as well as the direct use of the capacitance diaphragm gauge for the absolute pressure measurements enabled them to minimize the contributions to the relative uncertainty of the total EI cross sections arising from the absolute measurement of (b), (c), (d), and (e). Cross-section values with the lowest, at that moment, quoted rela-

tive uncertainty of 3.5% were obtained. Our present results and those of Straub *et al.* agree as regards the absolute values of the total cross sections at electron energies above 400 eV only. At lower energies the two data sets do not overlap within the combined relative standard uncertainties.

Among other measurements presented in Figs. 5–7, the early data of Smith [27] are incorrect [1,20]. The measurements of Wetzel *et al.* [19], Ma, Sporleder, and Bonham [21], Nagy, Skutlartz, and Schmidt [22], and Gaudin and Hagemann [23] reported relative uncertainties of 10–15% and therefore are not inconsistent with the present results. However, we note that the results of Wetzel *et al.* are systematically 15–20% higher than our data for all three rare gases. The results of Ref. [22] agree fairly well with our data

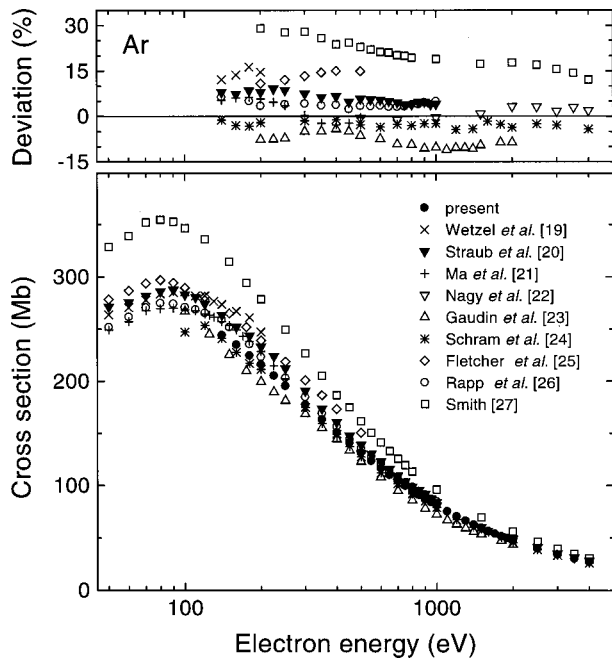


FIG. 5. Present total electron-impact ionization cross sections of Ar compared with published experimental data [19–27]. The upper plot shows the fractional deviation of these data from the present data.

for Ar and Xe, whereas considerable discrepancies in both the magnitude and the energy dependence of the cross sections exist for Kr. The data for Ar reported in Refs. [21] and [23] agree with our data within combined uncertainties, al-

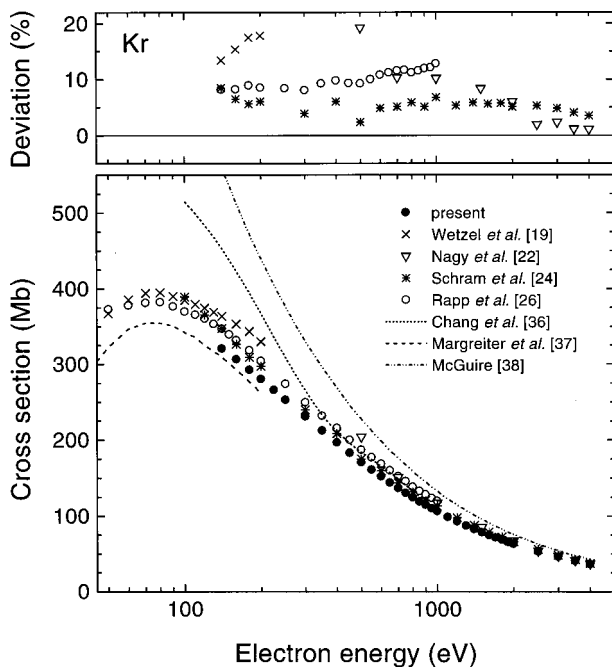


FIG. 6. Present total electron-impact ionization cross sections of Kr compared with published experimental data [19,22,24,26] and theoretical predictions [36–38]. The upper plot shows the fractional deviation of the published experimental data from the present data.

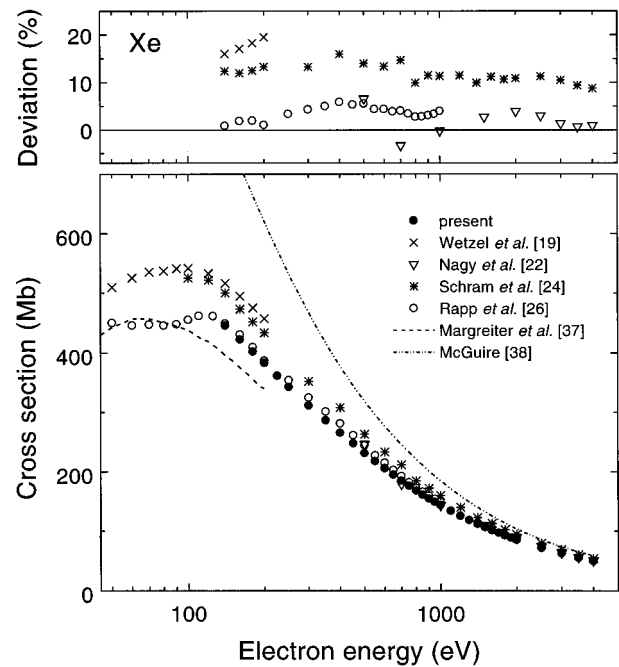


FIG. 7. Present total electron-impact ionization cross sections of Xe compared with published experimental data [19,22,24,26] and theoretical predictions [37,38]. The upper plot shows the fractional deviation of the published experimental data from the present data.

though the results of the latter group are approximately 10% smaller than ours.

The remaining measurements of Fletcher and Cowling [25] are reported with a relative uncertainty of 4.5%, although the results of this group for Ar are 11–15% higher than ours. We emphasize here that the results of Fletcher and Cowling are also higher than those of Straub *et al.* [20] and even of Rapp and Englander-Golden [26], although Fletcher and Cowling used an apparatus similar to that of Rapp and Englander-Golden.

Finally, taking into account our previous work concerning the measurements on Ne [1], we state that there is no experimental group whose results are in agreement with ours for all rare gases at the same time. Among the experimental data available for the absolute total EI cross sections, our data always confirm the lowest data set. Nevertheless, we emphasize that among others the results reported by Schram *et al.* [24], apart from Xe, appear to be in best agreement with our results.

In Figs. 6–8 we compare our total cross-section data for EI of Ar, Kr, and Xe with calculated data. The figures show recent results obtained for single ionization cross sections by Chang and Altick [36] using the distorted-wave Born approximation and by Margreiter, Deutsch, and Mark [37] using a semiclassical approach. Furthermore, we show three different calculations within the Born approximation made by McGuire [38], Omidvar, Kyle, and Suliva [39], and Wallace [40]. Only the results of Ref. [37] are in good agreement with our experimental data although it should be kept in mind that the authors made their calculation for single-ionization cross sections which are about 9% smaller than the total ones for Ar and Kr and 15% smaller for Xe [33].

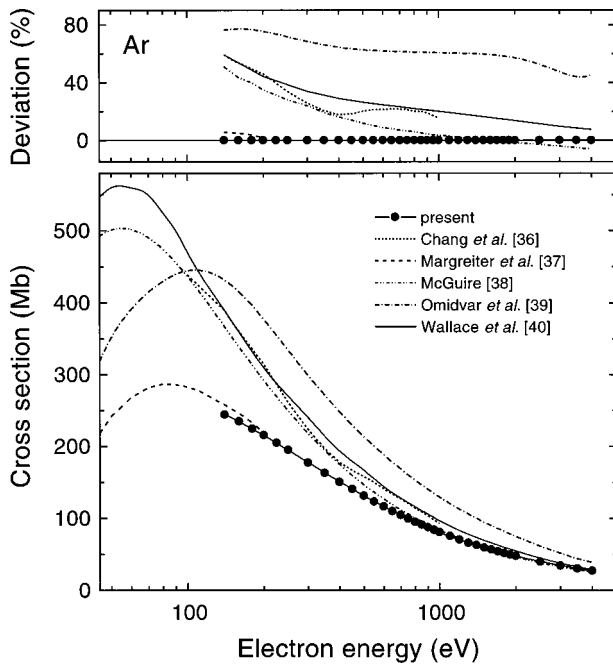


FIG. 8. Present total electron-impact ionization cross sections of Ar compared with theoretical predictions [36–40]. The upper plot shows the fractional deviation of these data from the present data.

However, we emphasize this agreement since these authors developed a simple analytical formula which is of great interest in many fields of applied research to reduce the calculation efforts. The quantum-mechanical calculations made within the Born approximation considerably overestimate our data, demonstrating that additional theoretical efforts must be made to obtain a consistent set of EI cross sections.

IV. CONCLUSION

We measured ratios of total electron-impact ionization cross sections to total photoionization cross sections of Ar, Kr, and Xe at an electron energy of 1000 eV and photon energies between 16 and 1012 eV. The measurements were performed at the NIM and SX700 beamlines in the radiometry laboratory of the Physikalisch-Technische Bundesanstalt at the electron storage ring BESSY I. Low relative standard uncertainties of 1.3–1.9% for the cross-section ratios were achieved. The measurements yield a common scale of total cross sections for EI and PI. Using the measured ratios and well-known PI cross sections, we deduced total EI cross sections of Ar, Kr, and Xe with a lowest relative standard uncertainty of 2% at an electron energy of 1000 eV, and of less than 2.2% at all other energies between 140 and 4000 eV, since elimination of the main uncertainties inherent in early cross-section measurements was achieved by our method. The high reliability of our results is confirmed by the good agreement of the data obtained at the two different beamlines in the two different spectral ranges. Our results considerably improve the database for absolute total EI cross sections, and hence for partial cross sections derived from these data. Moreover, our results also allow one to improve the database for total PI cross sections of Xe and Kr in the soft-x-ray spectral range.

ACKNOWLEDGMENTS

The authors are grateful to F. Scholze for fruitful discussions, and to U. Kroth for support during the experiments. This work was funded by the Deutsche Forschungsgemeinschaft (UI 156/1-1, 436 RUS 113/378/3), and by the Russian Foundation for Basic Research (96-02-00203G).

-
- [1] A. A. Sorokin, L. A. Shmaenok, S. V. Bobashev, B. Möbus, and G. Ulm, *Phys. Rev. A* **58**, 2900 (1998).
- [2] H. Rabus, V. Persch, and G. Ulm, *Appl. Opt.* **36**, 5421 (1997).
- [3] F. Scholze, H. Rabus, and G. Ulm, *J. Appl. Phys.* **84**, 2926 (1998).
- [4] F. Scholze, M. Krumrey, P. Müller, and D. Fuchs, *Rev. Sci. Instrum.* **65**, 3229 (1994).
- [5] A. Lau-Främbis, U. Kroth, H. Rabus, E. Tegeler, and G. Ulm, *Rev. Sci. Instrum.* **66**, 2324 (1995).
- [6] K. Solt, H. Melchior, U. Kroth, P. Kuschnerus, V. Persch, H. Rabus, M. Richter, and G. Ulm, *Appl. Phys. Lett.* **69**, 3662 (1996).
- [7] P. Kuschnerus, Ph.D. Thesis, TU Berlin, 1999 (unpublished).
- [8] J. A. R. Samson, *Phys. Rep., Phys. Lett.* **28C**, 303 (1976).
- [9] J. A. R. Samson, L. Lyn, G. N. Haddad, and G. C. Angel, *J. Phys. IV* **1**, C99 (1991).
- [10] B. X. Yang and J. Kirz, *Appl. Opt.* **26**, 3823 (1987).
- [11] W. S. Watson, *J. Phys. B* **5**, 2292 (1972).
- [12] D. R. Denne, *J. Phys. D* **3**, 1392 (1970).
- [13] B. L. Henke, R. L. Elgin, R. E. Lent, and R. B. Ledingham, *Norelco Reporter* **14**, 112 (1967).
- [14] F. Wuilleumier, Ph.D. Thesis, Université de Paris, 1969.
- [15] J. Lang and W. S. Watson, *J. Phys. B* **8**, L339 (1975).
- [16] J. A. R. Samson and L. Yin, *J. Opt. Soc. Am. B* **6**, 2326 (1989).
- [17] N. Saito and I. H. Suzuki, *Int. J. Mass Spectrom. Ion Processes* **115**, 157 (1992).
- [18] K. Codling and R. P. Madden, *J. Res. Natl. Bur. Stand., Sect. A* **76**, 1 (1972).
- [19] R. C. Wetzel, F. A. Baiocchi, T. R. Hayes, and R. S. Freund, *Phys. Rev. A* **35**, 559 (1987).
- [20] H. C. Straub, P. Renault, B. G. Lindsay, K. A. Smith, and R. F. Stebbings, *Phys. Rev. A* **52**, 1115 (1995).
- [21] C. Ma, C. R. Sporleder, and R. A. Bonham, *Rev. Sci. Instrum.* **62**, 909 (1991).
- [22] P. Nagy, A. Skutlartz, and V. Schmidt, *J. Phys. B* **13**, 1249 (1980).
- [23] A. Gaudin and R. Hagemann, *J. Chim. Phys. Phys.-Chim. Biol.* **64**, 1209 (1967).
- [24] B. L. Schram, F. J. De Heer, M. J. Van der Wiel, and J. Kistemaker, *Physica (Amsterdam)* **31**, 94 (1965); B. L. Schram, A. J. H. Boerboom, and J. Kistemaker, *ibid.* **32**, 185 (1966); B. L. Schram, *ibid.* **32**, 197 (1966); B. L. Schram, H. R. Moustafa, J. Schutten, and F. J. De Heer, *ibid.* **32**, 734 (1966).

- [25] J. Fletcher and I. R. Cowling, *J. Phys. B* **6**, L258 (1973).
- [26] D. Rapp and P. Englander-Golden, *J. Chem. Phys.* **43**, 1464 (1965).
- [27] P. T. Smith, *Phys. Rev.* **36**, 1293 (1930).
- [28] F. J. De Heer, R. H. J. Jansen, and W. Van der Kaay, *J. Phys. B* **12**, 979 (1979).
- [29] L. J. Kieffer and G. H. Dunn, *Rev. Mod. Phys.* **38**, 1 (1966).
- [30] T. D. Märk and G. H. Dunn, *Electron Impact Ionization* (Springer, Berlin, 1985).
- [31] K. Stephan, H. Helm, and T. D. Märk, *J. Chem. Phys.* **73**, 3763 (1980); K. Stephan and T. D. Märk, *ibid.* **81**, 3116 (1984).
- [32] K. Wiesemann, J. Puerta, and B. A. Huber, *J. Phys. B* **20**, 587 (1987); H. R. Koslowski, J. Binder, B. A. Huber, and K. Wiesemann, *ibid.* **20**, 5903 (1987); H. Lebius, J. Binder, H. R. Koslowski, K. Wiesemann, and B. A. Huber, *J. Phys. B* **22**, 83 (1989).
- [33] E. Krishnakumar and S. K. Srivastava, *J. Phys. B* **21**, 1055 (1988).
- [34] P. McCallion, M. B. Shah, and H. B. Gilbody, *J. Phys. B* **25**, 1061 (1992).
- [35] D. P. Almeida, A. C. Fontes, I. S. Mattos, and C. L. Godinho, *J. Electron. Spectrosc. Relat. Phenom.* **67**, 503 (1994); D. P. Almeida, A. C. Fontes, and C. F. L. Godinho, *J. Phys. B* **28**, 3335 (1995).
- [36] D. W. Chang and P. L. Altick, *J. Phys. B* **29**, 2325 (1996).
- [37] D. Margreiter, H. Deutsch, and T. D. Märk, *Int. J. Mass Spectrom. Ion Processes* **139**, 127 (1994).
- [38] E. J. McGuire, *Phys. Rev. A* **3**, 267 (1971); **16**, 62 (1977).
- [39] K. Omidvar, H. L. Kyle, and E. C. Sullivan, *Phys. Rev. A* **5**, 1174 (1972).
- [40] S. J. Wallace, R. A. Berg, and A. E. S. Green, *Phys. Rev. A* **7**, 1616 (1973).